The Crystal Structure of a Cummingtonite

By Subrata Ghose*

Department of Geology, University of Chicago, Chicago, U.S.A.

The crystal structure of a cummingtonite, $(Mg_{4.05}Fe_{2.50}Mn_{0.17}Ca_{0.35})(Si_{7.9}Al_{0.1})O_{22}(OH)_2$ (cell dimensions $a=9.51$, $b=18.19$, $c=5.33$ Å; $\beta=101°55'$; space group $C2/m$) has been refined by the least-squares method using three-dimensional Geiger counter intensity data and the parameters of grunerite as a starting point. The structure of cummingtonite is the same as that of tremolite, except that the curvature of the silicate double chains away from the plane of the metal atoms is more pronounced in cummingtonite. The M_4 position, corresponding to the calcium position in tremolite, is principally occupied by Fe^{2+}, the neighboring M_2 position principally by Mg^{2+}, while M_1 and M_3 positions are occupied by the rest of the Mg, Fe in a random manner. The short M_4–O_4 bond is probably covalent in character.

Introduction

Since the determination of the crystal structure of tremolite $(Ca_2Mg_5Si_8O_{22}(OH)_2)$ by Warren (1930), several varieties of amphibole, namely, crocidolite (Whittaker, 1949), actinolite and tremolite (Zussman, 1955, 1959), barroisitic hornblende and karinthine (Heritsch *et al.*, 1957) have been examined by two-dimensional Fourier methods for structural details. From the height of the electron-density peaks in the Fourier projection of crocidolite on (001), Whittaker (1949) deduced that M_2 position is richer in Fe^{3+}, and Mg rather than Fe enters the M_4 position. However, three-dimensional least-squares refinement of the structure of a grunerite with about 30 mol.% of the Mg component, derived from the metamorphosed iron formation of Quebec, Canada, indicated that M_4 position is mainly occupied by Fe^{2+}, while the rest of the Mg–Fe atoms are randomly distributed over the other three metal positions (Ghose & Hellner, 1959). Highly accurate structure determination of a cummingtonite, belonging to the same series as grunerite, and derived from the same locality, was therefore undertaken for two reasons. First, to determine the exact distribution of Mg–Fe over the four metal positions and secondly, to determine the exact configuration of the silicate double chains in an amphibole, where the M_4 position is occupied by a smaller cation (Mg^{2+}, Fe^{2+}), as opposed to Ca^{2+} or Na^+ as in tremolite, actinolite, crocidolite, etc. The cummingtonite series is unique in the amphibole group in that it contains very little aluminium and calcium or other alkali metals, and the beta angle is significantly different from the value found in other monoclinic amphiboles. It can be assumed from these two facts that the structure probably is not flexible enough to accommodate a large alkali ion and that the silicate chains are significantly distorted compared to those of

tremolite, for example. From the following structure determination, it will be seen that these assumptions are essentially correct.

Experimental

The specimen of the cummingtonite was collected by Dr R. F. Mueller from the metamorphosed iron formation, located approximately 180 miles north of Seven Islands, Quebec, near the Labrador boundary (for petrological details, see Mueller, 1960). The mineral occurs as pale brown needle shaped crystals, associated with quartz, dolomite and a little actinolite. A spectrochemical analysis of the cummingtonite by Dr Mueller is given in Table 1.

The formula of the cummingtonite can be written as:

$$(Mg_{4.05}Fe_{2.50}Mn_{0.17}Ca_{0.35})(Si_{7.9}Al_{0.1})O_{22}(OH)_2 .$$
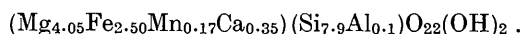
The calcium content has been attributed to the admixed actinolite by the analyst, Dr Mueller and has not been considered for the structure analysis.

The cell dimensions, listed below, have been measured by precession method, using Mo $K\alpha$ radiation.

$$a=9.51, \quad b=18.19, \quad c=5.33 \text{ Å}; \quad \beta=101°55'.$$
$$\text{Space group } C2/m. \quad Z=2 .$$

It should be noted that the standard orientation $C2/m$

Table 1. *Spectrochemical analysis of the cummingtonite*

	%
SiO_2	54.0
TiO_2	0.01
Al_2O_3	0.40
Fe	15.5
Fe_2O_3	*nd*
FeO	20.0
MnO	1.35
MgO	18.5
CaO	2.2
H_2O (calc.)	2.2

---

* Present address: Mineralogical Institute, University of Bern, Sahlistrasse 6, Bern, Switzerland.

has been chosen, rather than $I2/m$, which had been used for the description of amphibole structures since Warren (1930).

The intensity measurements were made on a cleavage fragment, ground to an ellipsoidal shape ($0\cdot2\times0\cdot2\times0\cdot3$ mm.), the longest axis being parallel to c. For obtaining high accuracy in the intensity measurements, a Geiger counter mounted on a Weissenberg type goniometer, along with monochromatic Mo $K\alpha$ radiation was used. The monochromatisation of the Mo $K\alpha$ radiation was effected by using a bent quartz crystal (Johansson type) monochromator. The experimental set up was very comparable to that used by Bommel & Bijvoet (1958) in their intensity measurements on ammonium hydrogen d-tartrate.

All the intensities, including the weak ones, occurring on six reciprocal lattice levels, perpendicular to c, having $\sin^2/\lambda^2$ below approximately $0\cdot36$ were measured by the Geiger counter. All the intensities were corrected for Lorentz, polarization and velocity factors by means of an Incor program (Zalkin & Jones, 1957) on the IBM 650 computer. No corrections for absorption, however, were made as they were believed to be small. The set of relative structure factors thus obtained, were put on an absolute basis by scaling them against the calculated structure factors, using the corresponding atomic parameters of grunerite. In the subsequent least-squares refinement, scale factor for each layer was treated as a variable parameter.

Three dimensional least-squares refinement

Atomic scattering curves for Si^{4+} and Mg^{2+} were taken from Berghuis et al. (1955). The atomic scattering curve for O taken from Berghuis et al. (1955) and that of Fe from Freeman (1959) were arbitrarily modified to take care of the ionization. Final atomic parameters of grunerite (Ghose & Hellner, 1959) were used as a starting point. Initially, the metals were given an average scattering factor of 62% $Mg^{2+}+38\%$ Fe^{2+}. The Least-Squares II program (Senko & Templeton, 1957) on an IBM 650 computer was used. Initially all the atoms were given a zero temperature factor and all the intensities were given a weight of unity. The unobserved intensities were assigned minimum F observed in each particular level concerned. For the initial stages of refinement, 739 intensities, having $\sin^2\theta/\lambda^2$ below $0\cdot22$, were considered. After two cycles of refinement, the temperature factor for the M_4 atom turned out to be negative, $-2\cdot18$, while those for M_1, M_2 and M_3 were $1\cdot32$, $2\cdot83$ and $1\cdot71$ respectively. The R-factor was $0\cdot196$. It was obvious that the M_4 position was very rich in Fe^{2+}, compared to the other three metal positions. So, a scattering curve of pure Fe^{2+} was used for the M_4 position, while an average scattering curve of the rest of the Mg^{2+}, Fe^{2+} was used for the other three positions for the next cycle. The R-factor decreased to $0\cdot158$ and the temperature factors were $-0\cdot27$ for M_1, $0\cdot28$ for M_2, $-0\cdot35$ for M_3 and $0\cdot72$ for M_4. After two cycles of refinement, including all the intensities, the R-factor decreased to $0\cdot145$, but the negative temperature factors for the M_1 and M_3 atoms still persisted and that of M_4 was much higher than the rest (atomic B: $M_1=-0\cdot31$, $M_2=0\cdot37$, $M_3=-0\cdot48$ and $M_4=1\cdot13$). This indicated that M_4 position has

Table 2. *Changes in the temperature factors of the metal atoms and the R-factors during the least-squares refinement*

Number of cycle	Program*	R-factors	\multicolumn{4}{c}{Temperature factors}	Remarks

Number of cycle	Program*	R-factors	M_1	M_2	M_3	M_4	Remarks
1	ST	0·196	1·32	2·82	1·71	−2·18	$f_M = Mg^{2+}_{0\cdot62}Fe^{2+}_{0\cdot38}$; 739 intensities considered
2	ST	0·158	−0·27	0·28	−0·35	0·72	$f_{M4}=$ pure Fe^{2+}; f_{M1},f_{M2}, $f_{M3}=Mg^{2+}_{0\cdot90}Fe^{2+}_{0\cdot10}$
3	ST	0·168	−0·32	0·34	−0·46	0·97	scattering curves same as above; 1524 intensities considered
4	ST	0·145	−0·31	0·37	−0·48	1·13	Same as above
5	ST	0·133	1·05	0·58	0·97	0·95	$f_{M1},f_{M3}=Mg^{2+}_{0\cdot67}Fe^{2+}_{0\cdot33}$; $f_{M2}=Mg^{2+}_{0\cdot90}Fe^{2+}_{0\cdot10}$; $f_{M4}=Mg^{2+}_{0\cdot20}Fe^{2+}_{0\cdot80}$
6	ST	0·131	1·12	0·64	1·07	1·09	Same as above
7	BL	0·123	0·97	0·99	0·90	0·71	$f_{M1},f_{M3}=Mg^{2+}_{0\cdot67}Fe^{2+}_{0\cdot33}$; $f_{M2}=Mg^{2+}_{0\cdot85}Fe_{0\cdot15}$; $f_{M4}=Mg^{2+}_{0\cdot25}Fe_{0\cdot75}$
8	BL	0·121	1·00	0·95	0·99	0·84	Same as above

* ST indicates Least Squares II program made by Senko & Templeton (1957) for the IBM 650 Computer.
BL indicates the full matrix least-squares program made by Busing & Levy (1959) for the IBM 704 Computer.

some Mg^{2+} in it and that M_1 and M_3 positions are richer in Fe^{2+} than was previously assumed. So at this stage Fe^{2+}, Mg^{2+} were distributed as follows: M_4 $=80\%$ Fe^{2+}, 20% Mg^{2+}; M_2 $=90\%$ Mg^{2+}, 10% Fe^{2+}; M_1 and M_3 $=67\%$ Mg^{2+}, 33% Fe^{2+}. Two more cycles of refinement brought the R-factor down to $0\cdot131$ and the temperature factors for the metal atoms were all positive; but the temperature factor for M_2 was lower than the rest. The metals were redistributed again, thus: $M_4=75\%$ Fe^{2+}, 25% Mg^{2+}; $M_2=85\%$ Mg^{2+}, 15% Fe^{2+}; M_1 and $M_3=67\%$ Mg^{2+}, 33% Fe^{2+}. Two more cycles of refinement on the IBM 704 computer using the full matrix least-squares program, made by Busing & Levy (1959), brought the R-factor down to $0\cdot121$ and the temperature factors for the metal atoms all turned out to be close to one. The weighting scheme used for this program was zero for the unobserved intensities and $1/F$ for the observed intensities. The changes in the isotropic temperature factors of the metal atoms in various cycles of least-squares refinement are listed in Table 2. So, it is seen that isotropic temperature factors serve as very good indicators of the kind of metal atom present in the four different metal positions. At this stage it was believed that the series had essentially converged, since the changes in the parameters were below the standard error. The final atomic parameters and isotropic temperature factors are listed in Table 3. A comparison of the observed structure factors with the structure factors calculated from the final parameters is shown in Table 4, a copy of which has been submitted to the American Documentation Institute*.

Table 3. *Atomic coordinates and temperature factors of cummingtonite*

	x	y	z	B
O_1	0·1129	0·0878	0·2056	0·82 Å²
O_2	0·1229	0·1713	0·7170	0·93
O_3	0·1135	0	0·7077	1·13
O_4	0·3789	0·2465	0·7740	1·35
O_5	0·3524	0·1312	0·0663	1·35
O_6	0·3484	0·1185	0·5616	1·37
O_7	0·3424	0	0·2696	1·17
Si_1	0·2880	0·0842	0·2747	0·73
Si_2	0·2976	0·1687	0·7819	0·76
M_1	0	0·0874	0·5000	1·00
M_2	0	0·1775	0	0·95
M_3	0	0	0	0·99
M_4	0	0·2598	0·5000	0·84

Accuracy of the determination

The standard deviations of the atomic parameters have been obtained by inverting the matrix of the

normal equations and are listed in Table 5. The average standard deviation of cation–oxygen bond length is $\pm 0\cdot007$ Å, that of oxygen–oxygen contacts is $\pm 0\cdot01$ Å. The average standard deviation of Si–O–Si angles is $\pm 0\cdot6°$ and that of O–Si–O angles is $\pm 0\cdot5°$. The limits of error in cation–oxygen distances, hence, are $\pm 0\cdot02$ Å, in oxygen–oxygen distances $\pm 0\cdot03$ Å, in Si–O–Si angles $\pm 1\cdot8°$ and in O–Si–O angles $\pm 1\cdot5°$.

Table 5. *Standard deviations of the atomic parameters of cummingtonite*

	$\sigma(x)$	$\sigma(y)$	$\sigma(z)$	$\sigma(B)$
O_1	0·00056	0·00026	0·00116	0·079 Å²
O_2	0·00057	0·00028	0·00127	0·082
O_3	0·00088	0	0·00176	0·119
O_4	0·00063	0·00032	0·00131	0·092
O_5	0·00065	0·00033	0·00114	0·101
O_6	0·00059	0·00031	0·00113	0·095
O_7	0·00085	0	0·00166	0·115
Si_1	0·00024	0·00011	0·00046	0·048
Si_2	0·00023	0·00011	0·00045	0·047
M_1	0	0·00014	0	0·054
M_2	0	0·00017	0	0·060
M_3	0	0	0	0·063
M_4	0	0·00009	0	0·046

Discussion of the structure

The metal atoms

From the course of the least-squares refinement, it is clear that the best agreement between observed and calculated structure factors is obtained, when we assume the following Mg^{2+}, Fe^{2+} distribution over the four different metal positions:

$$M_1 = M_3 = 67\% \ Mg^{2+}, \ 33\% \ Fe^{2+}$$
$$M_2 = 85\% \ Mg^{2+}, \ 15\% \ Fe^{2+}$$
$$M_4 = 75\% \ Fe^{2+}, \ 25\% \ Mg^{2+}.$$

The explanation that presents itself readily for this kind of Mg–Fe ordering is the difference in the ionic size of Mg^{2+} and Fe^{2+}. The M_4 position corresponds to the calcium position in tremolite structure and this position should accommodate the larger of the two ions, namely Fe^{2+}. However, the interatomic distances (Table 6) show that this explanation is not likely to be true. The M_4–O_4 bond distance is 2·04 Å, M_4–O_2 2·18 Å and M_4–O_6 is 2·70 Å.

The unusually short M_4–O_4 bond suggests that there might be covalent bonding between these two oxygens and M_4, which is mostly occupied by Fe^{2+}. These covalent bonds probably, are stabilizing this structure and favoring this type of Mg–Fe ordering in cummingtonite. If we examine the environment of the metal positions (Fig. 1), this explanation does not seem unreasonable. M_1 and M_3 are bonded to two (OH) ions and four oxygens, the oxygens being bonded to one silicon each. M_2 is bonded to six oxygens, which also are bonded to one silicon each. M_4, however, has a very distorted octahedral bonding. Four of the bonding oxygens, O_4 and O_2 are bonded to one silicon

Table 6. *Interatomic distances in cummingtonite* (Å)

M_1-O	M_1-O_1	2.07_7 (2)
	M_1-O_2	2.11_6 (2)
	M_1-O_3	2.10_4 (2)
	Mean	2.09_9
M_2-O	M_2-O_2	2.09_4 (2)
	M_2-O_1	2.12_9 (2)
	M_2-O_4	2.02_9 (2)
	Mean	2.08_4
M_3-O	M_3-O_1	2.10_2 (4)
	M_3-O_3	2.07_2 (2)
	Mean	2.09_2
M_4-O	M_4-O_4	2.04_2 (2)
	M_4-O_2	2.17_7 (2)
	M_4-O_6	2.69_9 (2)
	Mean	2.30_6

Si_1-O	Si_1-O_1	1.63_1
	Si_1-O_5	1.61_9
	Si_1-O_6	1.64_2
	Si_1-O_7	1.61_9
	Mean	1.62_8
Si_2-O	Si_2-O_2	1.62_7
	Si_2-O_4	1.61_7
	Si_2-O_5	1.64_6
	Si_2-O_6	1.63_8
	Mean	1.63_2
O–O around Si_1	O_1-O_5	2.65_8
	O_1-O_6	2.67_9
	O_1-O_7	2.67_0
	O_5-O_6	2.66_0, 2.69_4
	O_5-O_7	2.63_1
	O_6-O_7	2.65_3
	Mean	2.66_4

O–O around Si_2	O_2-O_4	2.75_5
	O_2-O_5	2.66_3
	O_2-O_6	2.63_6
	O_4-O_5	2.65_6
	O_4-O_6	2.57_9
	O_5-O_6	2.66_0, 2.69_4
	Mean	2.66_3
Si–Si	Si_1-Si_1'	3.06_3
	Si_1-Si_2	3.06_2, 3.09_6
	Si_2-Si_2	3.98_1
$M-M$	M_1-M_1'	3.17_9
	M_1-M_2	3.13_0
	M_1-M_3	3.10_4
	M_1-M_4	3.13_6
	M_2-M_3	3.22_8
	M_2-M_4	3.05_8

each, while two O_6 oxygens are shared between two silicons each and hence have their charges virtually satisfied. Since these two (O_6) oxygens are located at such a great distance from M_4, they make a rather weak charge contribution to the M_4 atom. The oxygen O_4 is unique, compared to O_1 or O_2, since it is bonded to one silicon and two metals, M_2 and M_4, while oxygens O_1 and O_2 are bonded to one silicon and three metals each. The short M_4-O_4 bond indicates that the linkage between M_4 and O_4 is stronger than a single $M-O$ bond.

Since Fe^{2+} is more electronegative than Mg^{2+}, O_2 and O_4 oxygens are strongly polarized by the M_4 atom, which is mostly Fe^{2+}. These four oxygens are also bonded to the M_2 atom. So that the structure may not be highly strained, it is expected that M_2 position will be occupied by a less electronegative atom, if it is available, in the present case Mg^{2+}.

The environments of M_1 and M_3 positions are very comparable and this is reflected in their metal contents, which are the same.
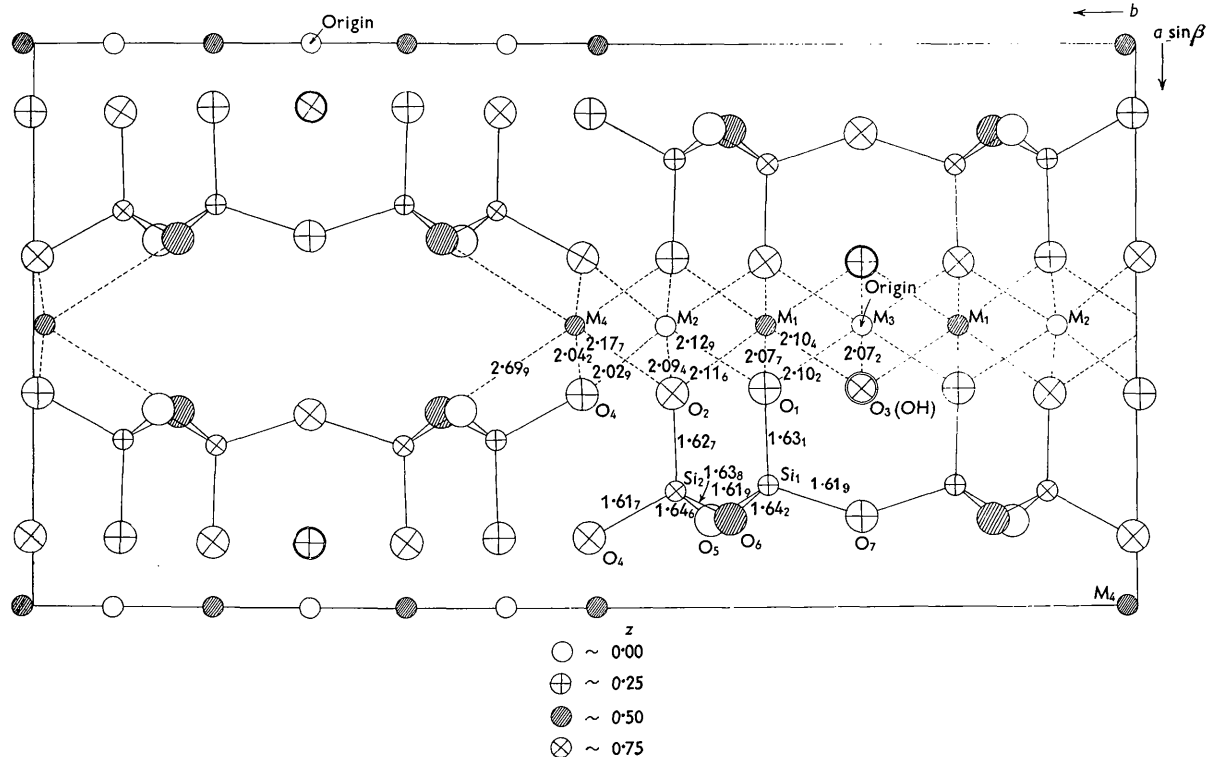
It is very probable that at a higher temperature,

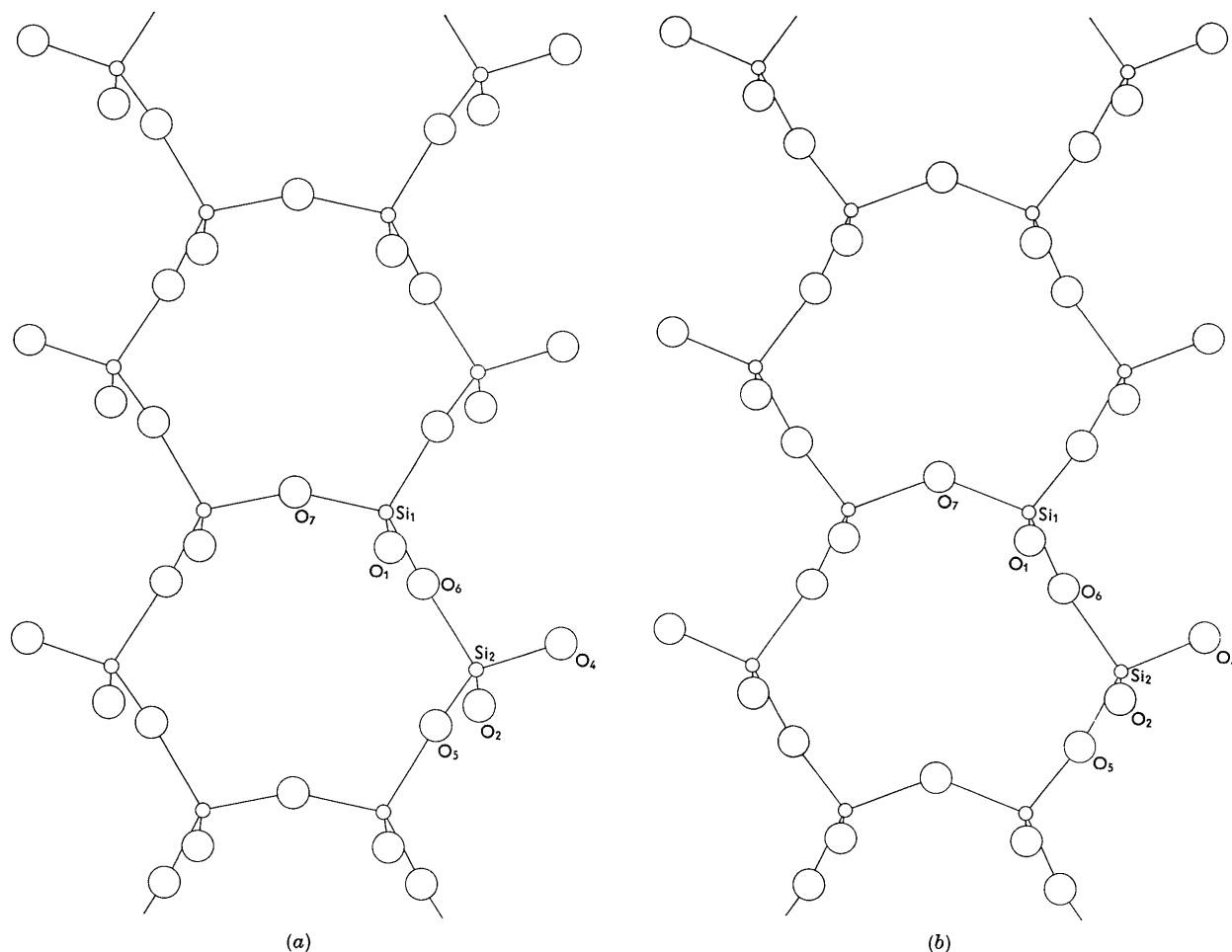Fig. 1. Projection of the structure of cummingtonite on (001).

(a)   (b)

Fig. 2. Orthogonal projection of the silicate double chains on (100) in $I2/m$ orientation in (a) cummingtonite; (b) tremolite; x, y parameters and cell dimensions from Zussman (1959), z parameter from Warren (1930).

the thermal vibrations will lengthen the M_4–O_4 bond and cause a disordering of Mg–Fe ions over all the four metal sites. Recently grunerite has been synthesized by Flaschen & Osborn (1957) by the breakdown of minnesotaite at 700 °C. and 17,500 psi. The magnesium end-member kupfferite, however, has not been synthesized yet. When more experimental data are available on this system, it may be possible to establish the degree of Mg–Fe ordering as a function of temperature in the cummingtonite series. In the absence of felspars, this may very well prove to be a geological thermometer, particularly for the metamorphosed iron formations.

The silicate chains

The silicate double chains are curved away from the plane of the metal atoms in cummingtonite, which has been noted also in other amphiboles, including tremolite. However, the chief difference between cummingtonite and other amphiboles is that in cummingtonite the M_4 position is occupied by Mg^{2+},

Fe^{2+} which are much smaller in size than C^{2+} or Na^+. So the oxygen atoms surrounding the M_4 position (except O_6) are much closer to M_4 in cummingtonite than they are in tremolite, crocidolite, hornblende, etc. The curvature of the silicate double chains, therefore, is more pronounced in cummingtonite than in other amphiboles. As explained by Whittaker (1949), this curvature arises out of the misfit in the repeat distances between free tetrahedral and free octahedral layers.

The silicate double chains in cummingtonite and in tremolite are shown in plan in Fig. 2(a), (b). It is noticed that the configuration of the silicate double chains in cummingtonite is somewhat different from that in tremolite. The distortion from the ideal hexagonal ring is effected by the clockwise rotation of both the SiO_4 tetrahedra in cummingtonite, while by the clockwise rotation of the Si_1–O tetrahedron and anticlockwise rotation of the Si_2–O tetrahedron in tremolite.

Whittaker (1949) and Zussman (1955) postulated

that the Si–O bond lengths within the silicon oxygen ring are larger than the peripheral bonds $Si_1–O_1$, $Si_2–O_2$ and $Si_2–O_4$ in crocidolite and actinolite. This is not true, however, in the case of cummingtonite.

Table 7. *Interatomic bond angles in cummingtonite*

Si–O–Si

$Si_1–O_5–Si_2$	142·9°, 139·4°
$Si_1–O_6–Si_2$	141·4
$Si_1–O_7–Si_1$	142·2
Mean	141·5°

$O–Si_1–O$

$O_7–Si_1–O_1$	110·5°
$O_6–Si_1–O_1$	109·9
$O_5–Si_1–O_1$	109·8
$O_7–Si_1–O_6$	108·8
$O_6–Si_1–O_5$	109·3
$O_5–Si_1–O_7$	108·6
Mean	109·5°

$O–Si_2–O$

$O_4–Si_2–O_2$	116·3°
$O_5–Si_2–O_2$	109·0
$O_6–Si_2–O_2$	107·7
$O_5–Si_2–O_6$	110·3
$O_6–Si_2–O_4$	104·7
$O_4–Si_2–O_5$	109·0
Mean	109·5°

Though the silicon–oxygen distances within two Si–O tetrahedra are not significantly different, the O–Si–O bond angles show that the Si_1–O tetrahedron is more regular, in which $O–Si_1–O$ bond angles range from 108·6° to 110·5°, while $O–Si_2–O$ bond angles range from 104·7° ($O_6–Si_2–O_4$) to 116·3° ($O_4–Si_2–O_2$). It may be noted that the two distorted tetrahedral angles in the Si_2–O tetrahedron involve O_4. The distortion in the Si_2–O tetrahedron, therefore, is

certainly caused by the strong attraction between O_4 and M_4.

The closest approach between oxygen atoms in two neighboring silicate chains is 2·97 Å. This distance is very comparable to those in crocidolite and actinolite, which are 2·97 and 2·9 Å.

References

BERGHUIS, J., HAANAPPEL, IJ. M., POTTERS, M., LOOPSTRA, B. O., MACGILLAVRY, C. H. & VEENENDAAL, A. L. (1955). *Acta Cryst.* 8, 478.
BOMMEL, A. J. VAN, & BIJVOET, J. M. (1958). *Acta Cryst.* 11, 61.
BUSING, W. R. & LEVY, H. A. (1959). Oak Ridge National Laboratory, Central Files Number 59-4-37.
FLASCHEN, S. S. & OSBORN, E. F. (1957). *Econ. Geol.* 52, 923.
FREEMAN, A. J. (1959). *Acta Cryst.* 12, 271.
GHOSE, S. & HELLNER, E. (1959). *J. Geol.* 67, 691.
HERITSCH, H., PAULITSCH, P. & WALITZI, E. M. (1957). *Tsch. Min. Pet. Mitt.* 6, 215.
MUELLER, R. F. (1960). *Amer. J. Sci.* 258, 449.
SENKO, M. E. & TEMPLETON (1957). *Acta Cryst.* 10, 385.
WARREN, B. E. (1930). *Z. Kristallogr.* 72, 42.
WHITTAKER, E. J. W. (1949). *Acta Cryst.* 2, 312.
ZALKIN, A. & JONES, R. E. (1957). *Acta Cryst.* 10, 385.
ZUSSMAN, J. (1955). *Acta Cryst.* 8, 385.
ZUSSMAN, J. (1959). *Acta Cryst.* 12, 309.

A Theoretical Study of Pendellösung Fringes.
Part 2. Detailed Discussion Based upon a Spherical Wave Theory

BY N. KATO

Division of Engineering and Applied Physics, Harvard University, Cambridge, Massachusetts, U.S.A.

Based upon the general formulation of Part 1, explicit expressions for the crystal wave fields and the vacuum wave fields are obtained assuming a spherical wave as the incident beam. For thick parts of crystals, absorption effects are taken into account. The same results as expected from the energy-flow theory (Kato, 1960) are obtained as a special case. 'Pendellösung' phenomena of X-rays are discussed. In particular, 'hook-shaped' patterns (Kato & Lang, 1959) can be fully explained. Values of integrated intensity according to the ordinary theory do not need to be revised.

1. Introduction

In Part 1 (Kato, 1960), we arrived at the conclusion that single-crystal diffraction in X-ray cases falls under a category in which (*a*) a spherical wave approximation is more appropriate, yet at the same time (*b*) the curvature of the wave surface of the incident